Proc. Natl. Acad. Sci. USA
Vol. 96, pp. 3281–3286, March 1999
Physiology

Insulin increases near-membrane but not global Ca^{2+} in isolated skeletal muscle

JOSEPH D. BRUTON*, ABRAM KATZ*†, AND HÅKAN WESTERBLAD*‡

Departments of *Physiology and Pharmacology and †Surgical Sciences, Karolinska Institute, 171 77 Stockholm, Sweden

Edited by Pedro M. Cuatrecasas, University of California School of Medicine, San Diego, CA, and approved January 5, 1999 (received for review August 28, 1998)

ABSTRACT **It has long been debated whether changes in Ca^{2+} are involved in insulin-stimulated glucose uptake in skeletal muscle. We have now investigated the effect of insulin on the global free myoplasmic Ca^{2+} concentration and the near-membrane free Ca^{2+} concentration ($[Ca^{2+}]_{mem}$) in intact, single skeletal muscle fibers from mice by using fluorescent Ca^{2+} indicators. Insulin has no effect on the global free myoplasmic Ca^{2+} concentration. However, insulin increases $[Ca^{2+}]_{mem}$ by ≈70% and the half-maximal increase in $[Ca^{2+}]_{mem}$ occurs at an insulin concentration of 110 microunits per ml. The increase in $[Ca^{2+}]_{mem}$ by insulin persists when sarcoplasmic reticulum Ca^{2+} release is inhibited but is lost by perfusing the fiber with a low Ca^{2+} medium or by addition of L-type Ca^{2+} channel inhibitors. Thus, insulin appears to stimulate Ca^{2+} entry into muscle cells via L-type Ca^{2+} channels. Wortmannin, which inhibits insulin-mediated activation of glucose transport in isolated skeletal muscle, also inhibits the insulin-mediated increase in $[Ca^{2+}]_{mem}$. These data demonstrate a new facet of insulin signaling and indicate that insulin-mediated increases in $[Ca^{2+}]_{mem}$ in skeletal muscle may underlie important actions of the hormone.**

Insulin exerts metabolic effects on tissues and defects in insulin action are associated with the existence of numerous diseases, including non-insulin-dependent diabetes mellitus, obesity, and hypertension (1). A defect in insulin-mediated glucose disposal in skeletal muscle is of particular significance because this tissue is responsible for removal of ≈90% of the glucose that disappears from the blood stream during hyperinsulinemia (2). Thus, understanding the process of insulin signaling in skeletal muscle is important. There is now considerable evidence that, subsequent to the binding of insulin to its receptor, a series of reactions involving protein phosphorylation and dephosphorylation, catalyzed by various protein kinases and phosphatases, occurs resulting in the metabolic effects of insulin (3). Additionally, changes in the intracellular concentrations of low molecular weight compounds (e.g., glucose 6-phosphate) (4), ions (5), and inositol phosphoglycans (3, 6) also appear to be involved in insulin signaling.

Whether insulin action involves changes in intracellular $[Ca^{2+}]$ is a long-standing debate (7, 8). Indirect evidence suggests that Ca^{2+} is involved in insulin action, particularly in glucose transport (8–10). Although one report shows that insulin increases intracellular $[Ca^{2+}]$ in adipocytes (11), most measurements of intracellular $[Ca^{2+}]$ in various cell types, including myotubes in culture, cardiac myocytes, and adipocytes, generally indicate no change in response to insulin (7, 12, 13). Therefore, it has been suggested that a minimal or permissive level of $[Ca^{2+}]$ is required for insulin actions (8, 9). It is surprising that the effect of insulin on intracellular $[Ca^{2+}]$ has not been investigated previously in this preparation, considering the importance of skeletal muscle in whole body glucose homeostasis (14). In the present study we used individual mouse skeletal muscle fibers to study the effect of insulin on global free myoplasmic calcium concentration ($[Ca^{2+}]_i$) and near-membrane free Ca^{2+} concentration ($[Ca^{2+}]_{mem}$).

MATERIALS AND METHODS

Materials. Insulin was from Novo-Nordisk, Copenhagen. FIP18 was from TEFLABS, Austin, TX. Indo-1 was from Molecular Probes Europe. Nifedipine and nimodipine were from Alamone Labs, Jerusalem. *N,N*-Dimethyltrimethylsilylamine was from Fluka, and diazoxide was from Tocris Cookson Ltd., Bristol, England. The remaining chemicals were from Sigma.

Fiber Mounting and Stimulation. Intact, single muscle fibers were isolated from the surface of the flexor brevis muscles of adult NMRI mice and mounted as described (15). To check that fibers were viable, tetanic contractions were produced by biphasic current pulses with an amplitude of 120–150% of the contraction threshold given at a frequency of 80 Hz. The fiber length was adjusted to the length giving maximum tetanic force. Fibers were usually stimulated only at the start and end of the experiment to avoid affecting the muscle's response to insulin application.

Solutions. Muscle fibers were superfused with a Tyrode solution containing 125 mM NaCl, 5 mM KCl, 0.5 mM $MgCl_2$, 0.4 mM Na_2PO_4, 1.8 mM $CaCl_2$, 1 mM EDTA, 25 mM $NaHCO_3$, and 5.5 mM glucose. Low Ca^{2+} solutions were prepared by replacing the $CaCl_2$ with 4 mM $MgCl_2$ in the above solution and then adding EGTA and calcium in appropriate amounts to give calculated free $[Ca^{2+}]$ of 1 or 20 nM (16). Fetal calf serum (0.2%) was added to all solutions, which were continuously bubbled with 95% O_2/5% CO_2 (pH 7.4). The temperature of the perfusate was 24–26°C. Insulin was added directly to the solution immediately before the experiments.

Ca^{2+} Measurements. Global $[Ca^{2+}]_i$ was measured with the fluorescent indicator Indo-1 as described (17). The indicator was pressure injected into fibers. $[Ca^{2+}]_{mem}$ was measured with a membrane-associating form of Indo-1, FIP18 (see ref. 18 for additional details). This indicator could be pressure injected only when the glass of the microelectrodes was silanized with *N,N*-dimethyltrimethylsilylamine. After the dye was injected, fibers were left for a further 40–60 min before any measurements were made. The two dyes were excited with light at 360 ± 5 nm, and the light emitted at 405 ± 5 and 490 ± 5 nm was measured with two photomultiplier tubes. The ratio (R) of the light emitted at 405 nm to that emitted at 490 nm was

The publication costs of this article were defrayed in part by page charge payment. This article must therefore be hereby marked "*advertisement*" in accordance with 18 U.S.C. §1734 solely to indicate this fact.

PNAS is available online at www.pnas.org.

This paper was submitted directly (Track II) to the *Proceedings* office.
Abbreviations: $[Ca^{2+}]_i$, myoplasmic free Ca^{2+} concentration; $[Ca^{2+}]_{mem}$, near-membrane free Ca^{2+} concentration; SR, sarcoplasmic reticulum.
‡To whom reprint requests should be addressed. e-mail: Hakan.Westerblad@fyfa.ki.se.

translated to $[Ca^{2+}]$ with the equation $[Ca^{2+}] = K_D\beta(R - R_{min})(R_{max} - R)^{-1}$, where K_D is the apparent dissociation constant of the dye, β is the ratio of the 490-nm signals at very low and saturating $[Ca^{2+}]$, and R_{min} and R_{max} are the ratios at very low and at saturating $[Ca^{2+}]$, respectively (19). Values for K_D, β, R_{min}, and R_{max} for Indo-1 and FIP18 were established intracellularly as described (20), with the exception that the *in vitro* K_D of FIP18 (450 nM) was used. The peak increase in $[Ca^{2+}]$ during 10 min of exposure to insulin was defined as the highest value achieved during a continuous 30-s interval.

Membrane Potential Measurements. A flat sheet containing about 15–20 muscle fibers was prepared from the flexor brevis muscles of adult NMRI mice. Fibers were penetrated with a microelectrode filled with KCl (1 M), and the potential difference between this electrode and a reference electrode filled with agar-KCl (1 M) was measured with a Geneclamp 500 amplifier (Axon Instruments, Foster City, CA) and displayed on an oscilloscope. In each preparation, the resting membrane potential was measured in four to six fibers in normal Tyrode solution and then after 8–20 min of exposure to 10 milliunits/ml insulin in another four to six fibers.

Statistics. Values are presented as means ± SEM. Statistical significance was determined with Student's paired or unpaired *t* tests as appropriate, and the significance level (*P*) was set at 0.05.

RESULTS

The initial experiments with the near-membrane Ca^{2+} indicator, FIP18, were performed to establish, first, that after injection the calcium-sensitive portion of the molecule was localized to the intracellular face of the sarcolemma and did not flip across the membrane to the outer surface and, second, that it responded to procedures known to elevate myoplasmic $[Ca^{2+}]$. The FIP18 signal was recorded in fibers before and during exposure to 1 mM Ni^{2+}, which is known to quench the

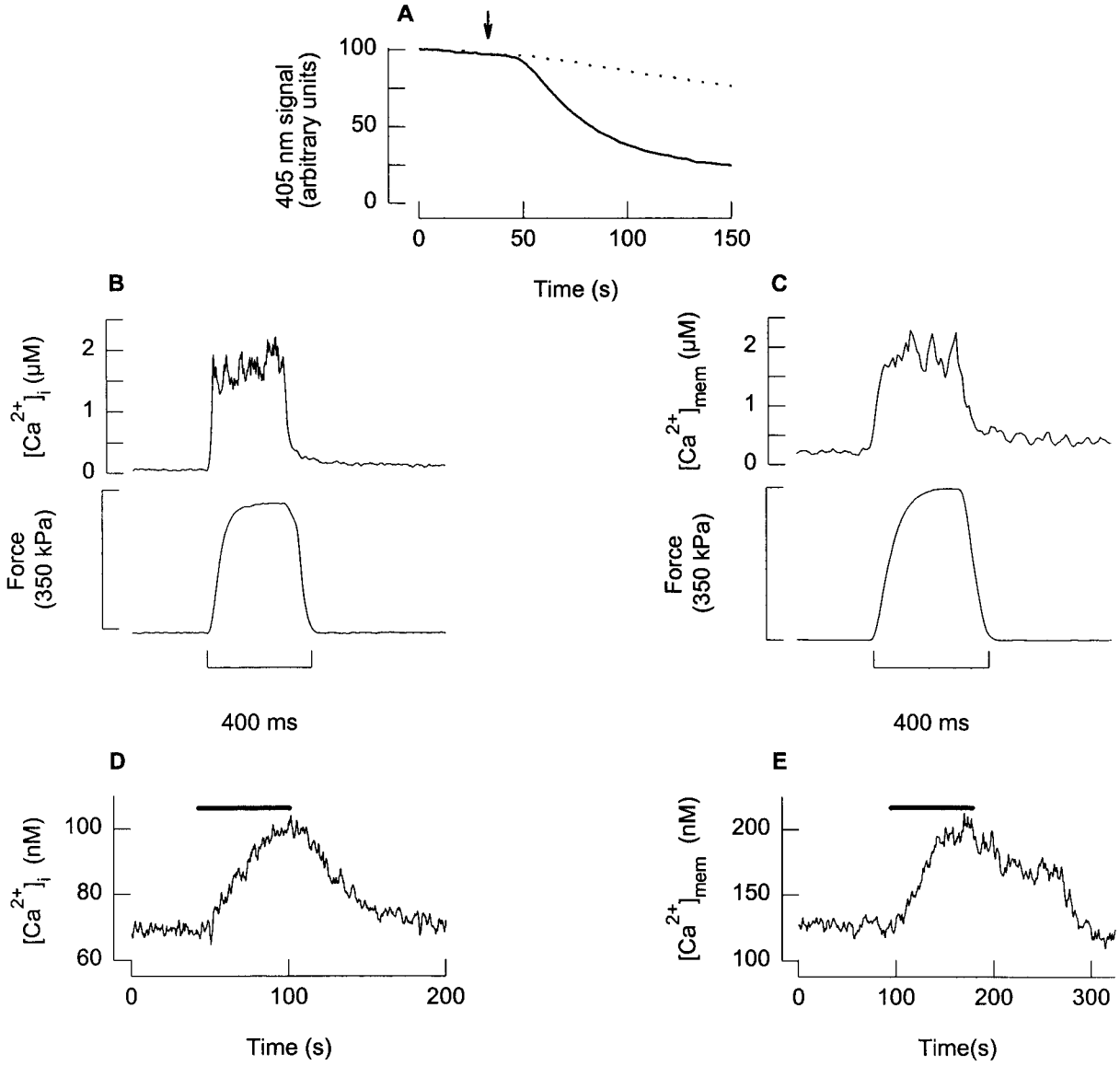

FIG. 1. Typical examples of the response of individual skeletal muscle fibers to exposure to Ni^{2+} or to electrical stimulation or caffeine. (*A*) FIP18 signal (405 nm of emitted light) before and during exposure to Ni^{2+} in an intact fiber (dotted line) or after a hole was created in its membrane, resulting in the interior of the fiber being exposed to the bathing solution (solid line); the arrow indicates the start of Ni^{2+} exposure. (*B*) Global $[Ca^{2+}]_i$ (measured with Indo-1) and the resultant force during an electrically induced tetanus. (*C*) $[Ca^{2+}]_{mem}$ (measured with FIP18) and the resultant force during an electrically induced tetanus. (*D*) Change in global $[Ca^{2+}]_i$ (measured with Indo-1) when 5 mM caffeine was applied. (*E*) Change in $[Ca^{2+}]_{mem}$ (measured with FIP18) when 5 mM caffeine was applied. Solid bars above records in *D* and *E* indicate the period of caffeine exposure.

fluorescent signal of calcium-sensitive dyes in their free and membrane-anchored forms (21). The FIP18 records shown in Fig. 1*A* demonstrate that, when the fiber was intact (dotted line), there was no change in the light emitted at 405 nm over a 200-s recording period, apart from a slow steady decline that was present even before application of Ni^{2+}. In contrast, when a hole was created in the fiber with a broken microelectrode and the interior of the fiber was exposed to the bathing solution (solid line), Ni^{2+} caused a clear decrease in the FIP18 signal. Similar results were obtained in another three fibers. These results indicate that the Ca^{2+}-sensitive portion of the FIP18 molecule faced the interior of the cell and did not reorientate itself across the cell membrane. In line with this, when external Ca^{2+} was decreased to <20 nM, there was no change in $[Ca^{2+}]_{mem}$ (data not shown). Fig. 1 *B–E* shows the response of fibers injected with either the global Ca^{2+} indicator Indo-1 or FIP18 to electrical stimulation or application of caffeine, which are known to cause Ca^{2+} release from the sarcoplasmic reticulum (SR) (22). The FIP18 signal clearly increased in response to both electrical stimulation (Fig. 1*B*) and application of 5 mM caffeine (Fig. 1*D*). Noteworthy is that basal $[Ca^{2+}]_{mem}$ (136 ± 26 nM, $n = 15$) is higher than basal $[Ca^{2+}]_i$ (61 ± 8, $n = 8$), which agrees with recent results in smooth muscle cells (18). Whereas the tetanic $[Ca^{2+}]$ detected with the two dyes were similar ($[Ca^{2+}]_i = 1.44 \pm 0.15$ μM, $n = 7$; $[Ca^{2+}]_{mem} = 1.56 \pm 0.28$ μM, $n = 6$), the increase in response to caffeine was larger for $[Ca^{2+}]_{mem}$ (140 ± 34 nM, $n = 10$) than for $[Ca^{2+}]_i$ (21 ± 6 nM, $n = 4$).

Global $[Ca^{2+}]_i$ averaged 61 nM before insulin exposure (see above) and did not change significantly during exposure to either 10 milliunits/ml insulin ($\Delta[Ca^{2+}]_i = -1.8 \pm 3.6$ nM, $n = 4$) or 100 milliunits/ml insulin ($\Delta[Ca^{2+}]_i = 2.5 \pm 0.9$ nM, $n = 4$) (Fig. 2*A*). However, 10 milliunits/ml insulin clearly increased $[Ca^{2+}]_{mem}$ (Fig. 2*B*), with the mean ± SEM increase of individual fibers averaging 71.9 ± 22.4% ($n = 15$; $P < 0.05$) at this insulin concentration. The insulin effect was reversible if insulin exposure was less than 10 min (Fig. 2*B*), and the effect was concentration dependent (Fig. 2*C*). A half-maximal increase in $[Ca^{2+}]_{mem}$ occurred at a calculated insulin concentration of 110 microunits/ml. The time course of the insulin-mediated increase of $[Ca^{2+}]_{mem}$ was measured in 20 fibers, and the time to reach half of the maximum increase was 2.51 ± 0.36 min.

Because the SR is the major intracellular storage site of Ca^{2+} in skeletal muscle, experiments were performed to determine whether the insulin-mediated increase in $[Ca^{2+}]_{mem}$ derived from the SR. Dantrolene, an inhibitor of SR Ca^{2+} release (23), was used to determine whether insulin altered $[Ca^{2+}]_{mem}$ by affecting SR Ca^{2+} release. Dantrolene (50 μM) significantly decreased the resting FIP18 ratio signal. This would be in part because of a reduced leak of Ca^{2+} from the SR and in part because of an artifact caused by altered light emission properties that resulted in a decrease of the ratio signal below R_{min}. Thus, the ratio signals in the presence of dantrolene cannot be converted into $[Ca^{2+}]_{mem}$. However, dantrolene did not block the insulin-mediated increase in FIP18 ratio, i.e., $[Ca^{2+}]_{mem}$ (Fig. 3*A*). Similar results were obtained in a further three fibers with a mean change in the FIP18 ratio of 0.306 ± 0.112 compared with a mean change of 0.200 ± 0.116 in the absence of dantrolene, indicating that insulin does not stimulate Ca^{2+} release from a dantrolene-sensitive SR Ca^{2+} pool. Noteworthy is that, although dantrolene does not block the insulin-mediated increase in the FIP18 ratio, dantrolene does block the ability of insulin to increase the ratio above basal.

Insulin had little effect on tetanic force (Fig. 3*B*) and tetanic $[Ca^{2+}]_i$ (Fig. 3*C*). Data from four fibers showed no significant effect of insulin (10 milliunits/ml) on either tetanic force (99.5 ± 2.2% of control) or tetanic $[Ca^{2+}]_i$ (95.2 ± 6.5% of control). Thus, insulin does not appear to stimulate voltage-activated SR Ca^{2+} release. An alternative mechanism by which

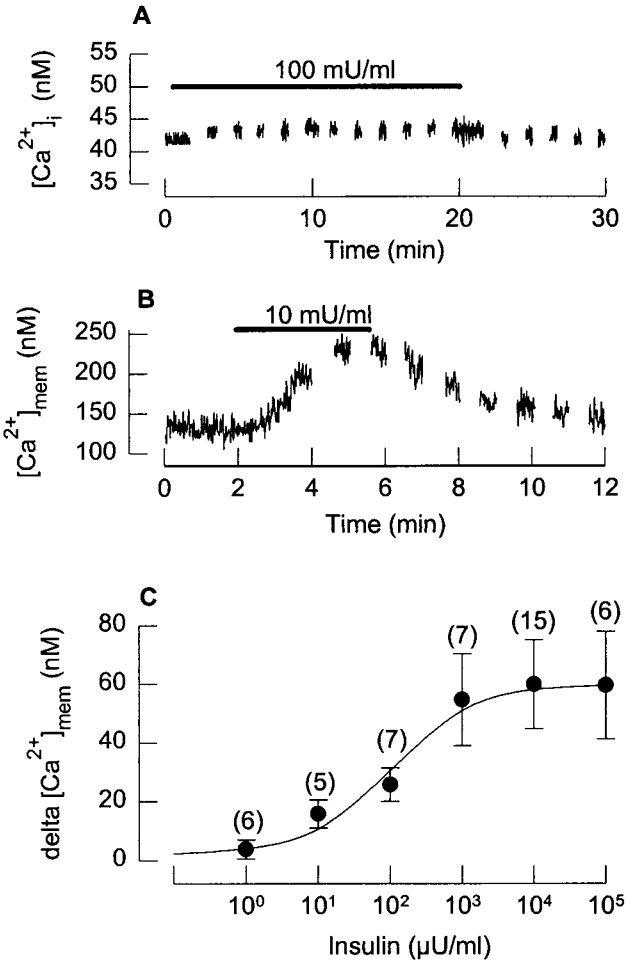

FIG. 2. Insulin increases calcium only near the membrane. (*A*) Global $[Ca^{2+}]_i$ (measured with Indo-1) shows little change when insulin is applied (indicated by solid bar). (*B*) $[Ca^{2+}]_{mem}$ (measured with FIP18) increases when insulin is applied (shown by solid bar). Gaps in records *A* and *B* are when light was switched off to avoid bleaching of the dye. (*C*) Insulin dose–effect curve showing the increase in near-membrane calcium when increasing concentrations of insulin were applied. Values are means ± SEM, and the number of fibers is indicated for each point. The curve was drawn by fitting a sigmoidal function to the data points.

insulin can increase $[Ca^{2+}]_{mem}$ is by inhibiting SR Ca^{2+} uptake. Changes of SR Ca^{2+} uptake can be assessed by analyzing $[Ca^{2+}]_i$ tails after tetani, i.e., the slow, late phase of Ca^{2+} decay after a tetanus (17). Typical examples of the $[Ca^{2+}]_i$ tail in the presence and absence of insulin are shown in Fig. 3*D*. It can be seen that insulin had no marked effect on these tails. Similar results were obtained in three other fibers in which $[Ca^{2+}]_i$ tails were studied, and hence there is no indication of an insulin-mediated effect on SR Ca^{2+} uptake. Taken together, these results indicate that insulin does not increase $[Ca^{2+}]_{mem}$ by altering SR function.

Subsequent experiments were aimed at determining whether the increase of $[Ca^{2+}]_{mem}$ with insulin was caused by influx of Ca^{2+} from the extracellular fluid. The $[Ca^{2+}]_{mem}$ increase with insulin was somewhat attenuated (not significant) when the extracellular $[Ca^{2+}]$ was reduced to 20 nM (Fig. 4). When insulin was applied at 1 nM extracellular Ca^{2+}, the increase of $[Ca^{2+}]_{mem}$ was small and significantly smaller than the increase at normal extracellular Ca^{2+}. Thus, the insulin-mediated increase of $[Ca^{2+}]_{mem}$ was reduced when the inward driving force for Ca^{2+} was reduced or reversed, suggesting that insulin was stimulating Ca^{2+} entry into muscle cells. In six

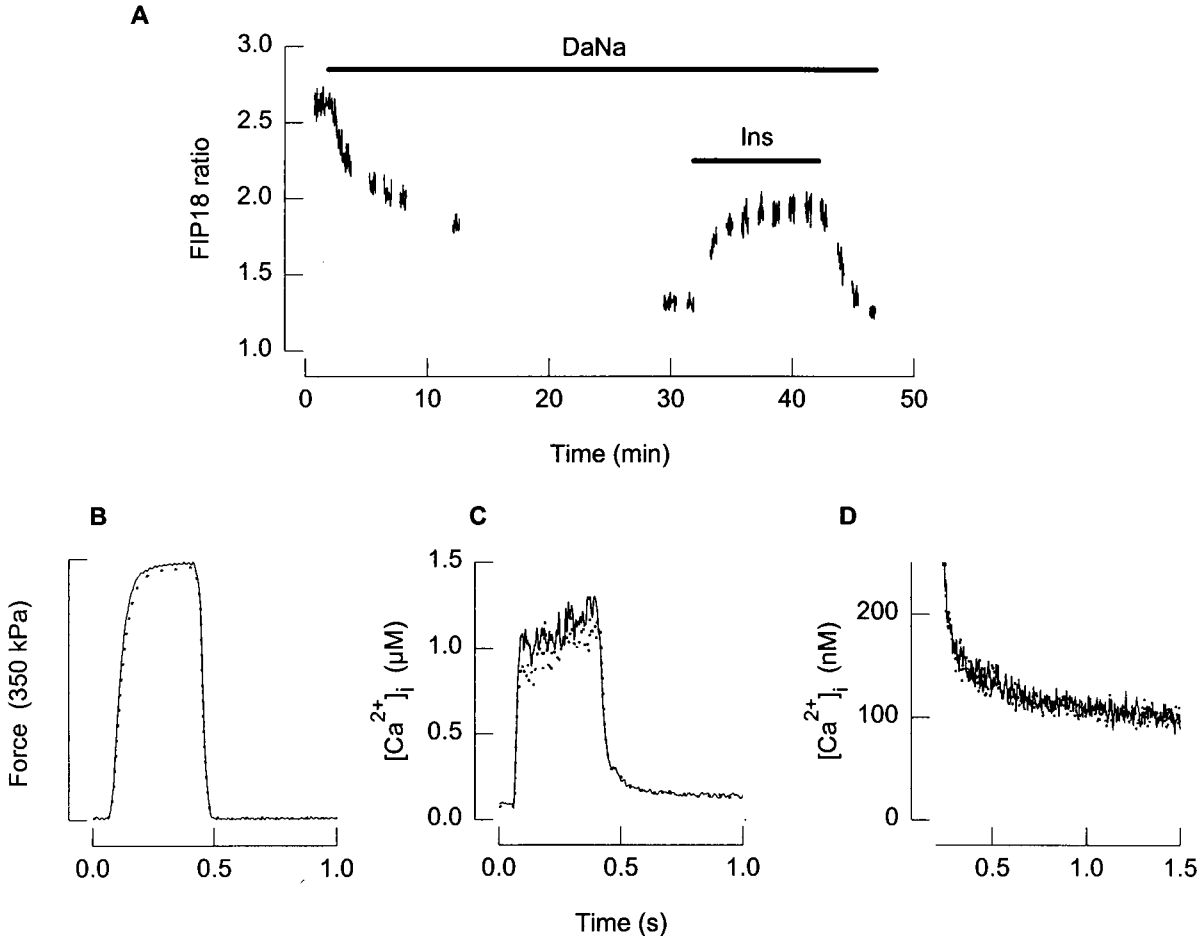

FIG. 3. The source of the insulin-stimulated increase in near-membrane calcium is not the SR. (*A*) Dantrolene sodium causes a reduction in the FIP18 ratio but does not block the insulin-stimulated increase in the FIP18 ratio. The solid bars indicate application of 50 μM dantrolene sodium (DaNa) or 10 milliunits/ml insulin (Ins). Gaps in record *A* are when light was switched off to avoid bleaching of the dye. Insulin (10 milliunits/ml) had little effect on tetanic force (*B*), tetanic $[Ca^{2+}]_i$ (*C*; measured with Indo-1), or the tail of $[Ca^{2+}]_i$ after the tetanus (*D*). The solid lines in *B–D* indicate records obtained in control solution, and dotted lines indicate records after 15 min of exposure to 10 milliunits/ml insulin.

fibers, 5 mM caffeine increased $[Ca^{2+}]_{mem}$ by 133 ± 49 nM in the presence of 1 nM extracellular Ca^{2+}, and this was not significantly different from the increase of 140 ± 34 nM obtained in 10 fibers exposed to the same concentration of caffeine in 1.8 mM extracellular Ca^{2+}. Therefore, during exposure of the fiber to low extracellular Ca^{2+}, SR still contained Ca^{2+} and was able to release it in sufficient quantities to bind to the membrane-bound FIP18 dye. This demonstrates that the lack of increase in $[Ca^{2+}]_{mem}$ in response to insulin after removal of extracellular Ca^{2+} is not caused by Ca^{2+} depletion of SR.

To determine the mode of insulin-stimulated Ca^{2+} entry, the effects of either nifedipine or nimodipine, both L-type Ca^{2+} channel blockers (24, 25) on $[Ca^{2+}]_{mem}$ were studied. L-type channels were considered because blockers of these channels inhibit insulin-mediated glucose transport in isolated skeletal muscle (24, 26). Application of these Ca^{2+} channel blockers significantly reduced the insulin-mediated increase in $[Ca^{2+}]_{mem}$ (Fig. 4), suggesting that insulin application resulted in the opening of L-type Ca^{2+} channels.

Insulin has long been known to hyperpolarize skeletal muscle cells, and in agreement with this, we found that 10 milliunits/ml insulin caused a small but significant hyperpolarization averaging 3 mV (n = 26 fibers). The hyperpolarization is believed to result from increased activity of the Na-K ATPase pump (27). However, opening of the inwardly rectifying K channel that exists in skeletal muscle may also contribute. Recently, it was suggested that the K_{ATP} channel present in both pancreatic beta cells and skeletal muscle might be involved in insulin action (28). To test this hypothesis, we exposed muscle fibers to 250 μM diazoxide [a known activator of K_{ATP} channels (29)] for 5 min before addition of 10 milliunits/ml insulin. In five fibers so treated, the mean increase in $[Ca^{2+}]_{mem}$ was not significantly different from the increase induced by insulin alone (Fig. 4).

Finally, the effect of wortmannin, an inhibitor of insulin- but not contraction-mediated glucose transport (30, 31), on the insulin-mediated increase of $[Ca^{2+}]_{mem}$ was studied. Wortmannin significantly reduced the increase of $[Ca^{2+}]_{mem}$ with insulin (Fig. 4) but had no effect on tetanic force or tetanic $[Ca^{2+}]_i$ (data not shown).

DISCUSSION

The main result of the present study is that insulin application significantly increases the $[Ca^{2+}]$ close to the membrane ($[Ca^{2+}]_{mem}$) of muscle cells but has no effect on global $[Ca^{2+}]_i$. If insulin caused a significant uniform increase in $[Ca^{2+}]_i$ throughout the myoplasm, this could potentially be counterproductive, because of activation of Ca^{2+}-dependent protein kinases (e.g., phosphorylase kinase) in the cell interior, which would result in glycogenolysis and inhibition of glucose utilization (32). Insulin, on the other hand, stimulates glycogen synthesis while preventing glycogenolysis in muscle (33). Indeed, others have shown that insulin-stimulated glucose uptake in adipocytes is decreased at high intracellular $[Ca^{2+}]$

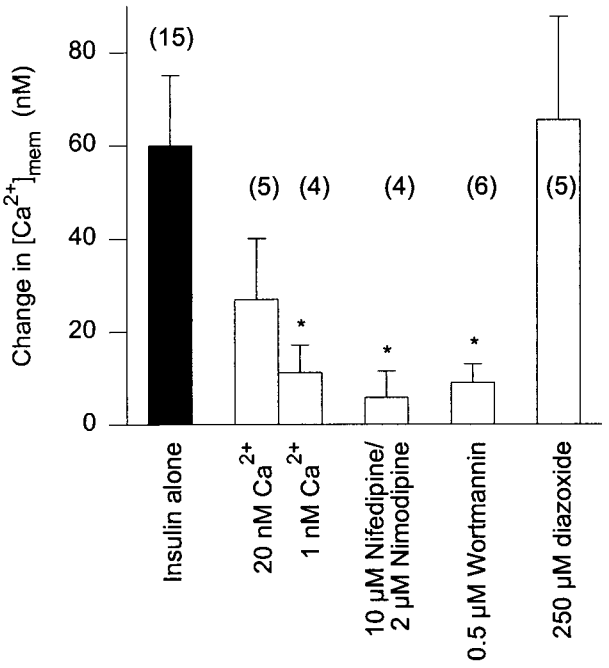

FIG. 4. The effect of decreasing extracellular Ca^{2+}, the addition of L-type Ca^{2+} channel blockers, diazoxide, or wortmannin on the insulin-stimulated increase in $[Ca^{2+}]_{mem}$. Insulin was present in all experiments at 10 milliunits/ml. Unless noted otherwise, extracellular calcium was 1.8 mM. Values are means ± SEM, and the number of observations is shown in parentheses. An asterisk indicates when the response was significantly smaller ($P < 0.05$) than the response to insulin alone.

(34), which presumably primarily reflects cytosolic $[Ca^{2+}]$. Moreover, a substantial increase of $[Ca^{2+}]_i$ would result in activation of the contractile machinery and, subsequently, contracture. The threshold for contraction in this preparation is about 200–300 nM $[Ca^{2+}]_i$ (17). The finding that insulin increases $[Ca^{2+}]_{mem}$ but not global $[Ca^{2+}]_i$ may explain why previous investigators generally failed to detect changes in intracellular $[Ca^{2+}]$ after exposure to insulin.

The physiological significance of the insulin-mediated increase of $[Ca^{2+}]_{mem}$ is addressed as follows. First, the insulin concentration that yielded the half-maximal increase in $[Ca^{2+}]_{mem}$ was 110 microunits/ml, with saturation being achieved at ≈1,000 microunits/ml (Fig. 2*C*). These values are similar to those for insulin-mediated activation of glucose transport in isolated mouse skeletal muscle (half-maximal insulin concentration ≈130 microunits/ml, saturating ≈1,100 microunits/ml) (35), as well as insulin-mediated activation of whole body and forearm (i.e., muscle) glucose uptake during euglycemic (5 mM) hyperinsulinemia in man (36). Second, Ca^{2+} channel blockers (24), wortmannin (30, 31), and removal of extracellular Ca^{2+} (10), all of which inhibit insulin-mediated glucose transport in muscle, inhibit the insulin-mediated increase in $[Ca^{2+}]_{mem}$. Last, dantrolene, which inhibits insulin-mediated glucose transport in isolated skeletal muscle (8), blocks the ability of insulin to increase the FIP18 ratio signal (i.e., $[Ca^{2+}]_{mem}$) above basal (Fig. 3*A*). These findings suggest that the increase in $[Ca^{2+}]_{mem}$ above basal is an important step in the insulin-mediated activation of glucose transport in skeletal muscle.

Results with low extracellular Ca^{2+} solutions and blockers of the L-type Ca^{2+} channels suggest that the increase in $[Ca^{2+}]_{mem}$ is a consequence of Ca^{2+} influx, presumably through L-type Ca^{2+} channels in the sarcolemma. Because the L-type Ca^{2+} channels primarily reside in the transverse tubules (23) and FIP18 probably reflects the near-membrane Ca^{2+} concentration also in the surface membrane, it is possible that we are underestimating the true local increase in $[Ca^{2+}]_{mem}$. The precise mechanism by which insulin causes an influx of Ca^{2+} is not clear. Clearly, it is not by voltage activation of Ca^{2+} channels because insulin hyperpolarizes rather than depolarizes muscle fibers. One possibility is that Ca^{2+} channels are activated by one of the many protein kinases that exist in their vicinity (37).

Because insulin mediates its effects by first binding to its receptor, it might be argued that extracellular Ca^{2+} is needed for insulin binding. Therefore, the reduced insulin response in low extracellular Ca^{2+} may be explained by insufficient insulin binding rather than by a decrease in Ca^{2+} entry. Although removal of extracellular Ca^{2+} was shown to decrease insulin binding in isolated rat muscle by ≈30% (38), it is unlikely that such a decrease in insulin binding substantially compromised insulin signaling. This is supported by the finding that essential depletion of extracellular Ca^{2+} did not markedly alter the extent of glycogen synthase activation by insulin in muscle cell cultures (39). These observations, together with the present findings that blockers of the L-type Ca^{2+} channels attenuate the insulin response, favor an influx of Ca^{2+} rather than impaired insulin binding to its receptor as being the major mechanism whereby Ca^{2+} is involved in insulin signaling.

The insulin-mediated increase in $[Ca^{2+}]_{mem}$ is markedly reduced by exposing the fibers to wortmannin, which inhibits phosphatidylinositol 3-kinase. This might mean that the insulin effect on $[Ca^{2+}]_{mem}$ is mediated by phosphatidylinositol 3-kinase, which is an early intermediate in insulin-mediated but not contraction-mediated glucose transport in skeletal muscle (30, 31). However, in addition to phosphatidylinositol 3-kinase, wortmannin also inhibits other enzymes (40), which may be involved in the insulin-mediated increase of $[Ca^{2+}]_{mem}$.

There is now considerable evidence that intracellular Ca^{2+} gradients exist in cells under certain conditions (18, 41–43), and the current findings are consistent with such data. Although it is currently not clear whether the insulin-induced increase in $[Ca^{2+}]_{mem}$ plays a role in the activation of glucose transport, it is possible that Ca^{2+} is involved in the docking and insertion of glucose transport proteins (Glut4) receptors into the cell membrane, as in the Ca^{2+}-dependent docking of synaptic vesicles in nerve terminals (44).

This work was supported by grants from the Swedish Medical Research Council (Project 10842), the Swedish National Center for Sports Research, Magnus Bergvalls Foundation, and Novo Nordisk Fonden and funds at the Karolinska Institutet.

1. Borkman, M., Storlein, L. H., Pan, D. A., Jenkins, A. B., Chisholm, D. J. & Campbell, L. V. (1993) *N. Engl. J. Med.* **328,** 238–244.
2. DeFronzo, R. A., Gunnarsson, R., Björkman, O., Olsson, M. & Wahren, J. (1985) *J. Clin. Invest.* **76,** 149–155.
3. Saltiel, A. R. (1996) *Am. J. Physiol.* **270,** E375–E385.
4. Villar-Palasi, C. & Guinovart, J. J. (1997) *FASEB J.* **11,** 544–558.
5. Draznin, B. & Reusch, J. E.-B. (1996) in *Diabetes Mellitus*, eds. Leroith, D., Taylor, S. I. & Olefsky, J. M. (Lippincott-Raven, Philadelphia), pp. 227–234.
6. Romero, G. & Larner, J. (1993) *Adv. Pharmacol.* **24,** 21–50.
7. Klip, A. & Ramlal, T. (1987) *J. Biol. Chem.* **262,** 9141–9146.
8. Youn, J. H., Gulve, E. A., Henriksen, E. J. & Holloszy, J. O. (1994) *Am. J. Physiol.* **267,** R888–R894.
9. Pershadsingh, H. A., Shade, D. L., Delfert, D. M. & McDonald, J. M. (1987) *Proc. Natl. Acad. Sci. USA* **84,** 1025–1029.
10. Schudt, C., Gaertner, U. & Pette, D. (1976) *Eur. J. Biochem.* **68,** 103–111.
11. Draznin, B., Kao, M. & Sussman, K. E. (1987) *Diabetes* **36,** 174–178.
12. Cheung, J. Y., Constantine, J. M. & Bonventre, J. V. (1987) *Am. J. Physiol.* **252,** C163–C172.
13. Kelly, K. L., Deeney, J. T. & Corkey, B. E. (1989) *J. Biol. Chem.* **264,** 12754–12757.

14. Mueckler, M. & Holman, G. (1995) *Nature (London)* **377,** 100–101.
15. Lännergren, J. & Westerblad, H. (1987) *J. Physiol. (London)* **390,** 285–293.
16. Bers, D. M., Patton, C. W. & Nuccitelli, R. (1994) *Methods Cell Biol.* **40,** 3–29.
17. Westerblad, H. & Allen, D. G. (1994) *J. Physiol. (London)* **474,** 291–301.
18. Etter, E. F., Minta, A., Poeni, M. & Fay, F. S. (1996) *Proc. Natl. Acad. Sci. USA* **93,** 5368–5373.
19. Grynkievicz, G., Poenie, M. & Tsien, R. Y. (1985) *J. Biol. Chem.* **260,** 3440–3450.
20. Andrade, F. H., Reid, M. B., Allen, D. G. & Westerblad, H. (1998) *J. Physiol. (London)* **509,** 565–575.
21. Davies, E. V. & Hallett, M. B. (1996) *Cell Calcium* **19,** 355–362.
22. Allen, D. G. & Westerblad, H. (1995) *J. Physiol. (London)* **487,** 331–342.
23. Fleischer, S. & Makato, I. (1989) *Annu. Rev. Biophys. Biophys. Chem.* **18,** 333–364.
24. Cartee, G. D., Briggs-Tung, C. & Holloszy, J. O. (1992) *Am. J. Physiol.* **263,** R70–R75.
25. Cerbai, E., Gotti, A. & Mugelli, A. (1997) *Br. J. Pharmacol.* **120,** 667–675.
26. Young, J. C. & Balon, T. W. (1997) *Life Sci.* **61,** 335–342.
27. Clausen, T. & Flatman, J. (1987) *Am. J. Physiol.* **252,** E492–E499.
28. Miki, T., Nagashima, K., Tashiro, F., Kotake, K., Yoshitomi, H., Tamamoto, A., Gonoi, T., Iwanaga, T., Miyazaki, J.-I. & Seino, S. (1998) *Proc. Natl. Acad. Sci. USA* **95,** 10402–10406.
29. Miura, Y., Henquin, J. C. & Gilon, P. (1997) *J. Physiol. (London)* **503,** 387–398.
30. Lee, A. D., Hansen, P. A. & Holloszy, J. O. (1995) *FEBS Lett.* **361,** 51–54.
31. Yeh, J.-I., Gulve, E. A., Rameh, L. & Birnbaum, M. J. (1995) *J. Biol. Chem.* **270,** 2107–2111.
32. Katz, A., Sahlin, K. & Broberg, S. (1991) *Am. J. Physiol.* **260,** E411–E415.
33. Challiss, R. A. J., Crabtree, B. & Newsholme, E. A. (1987) *Eur. J. Biochem.* **163,** 205–210.
34. Draznin, B., Sussman, K., Kao, M., Lewis, D. & Sherman, N. (1987) *J. Biol. Chem.* **262,** 14385–14388.
35. Le Marchand-Brustel, Y. & Freychet, P. (1979) *J. Clin. Invest.* **64,** 1505–1515.
36. Yki-Jarvinen, H., Mott, D., Young, A. A., Stone, K. & Bogardus, C. (1987) *J. Clin. Invest.* **80,** 95–100.
37. Gray, P. C., Tibbs, V. C., Catterall, W. A. & Murphy, B. J. (1997) *J. Biol. Chem.* **242,** 6297–6302.
38. Gould, M. K. & Chaudry I. H. (1970) *Biochim. Biophys. Acta* **215,** 249–257.
39. Gaertner, U., Schudt, C. & Pette, D. (1977) *Mol. Cell. Endocrinol.* **8,** 35–46.
40. Cross, M. J., Stewart, A., Hodgkin, M. N., Kerr, D. J. & Wakelam, M. J. O. (1995) *J. Biol. Chem.* **270,** 25352–25355.
41. Golovina, V. A. & Blaustein, M. P. (1997) *Science* **275,** 1643–1648.
42. Petersen, O. H., Petersen, C. C. H. & Kasai, H. (1994) *Annu. Rev. Physiol.* **56,** 297–319.
43. Marrion, N. V. & Tavalin, S. J. (1998) *Nature (London)* **395,** 900–905.
44. Jahn, R. & Sudhof, T. C. (1994) *Annu. Rev. Neurosci.* **17,** 219–246.